Supporting Information

Rare-earth metal-promoted (double) C–H-bond activation of a lutidinyl-functionalized alkoxy ligand: formation of [ONC] pincer-type ligands and implications for isoprene polymerization

Dominic Diether,[a] Melanie Meermann-Zimmermann,[a,b] Karl W. Törnroos,[b] Cäcilia Maichle-Mössmer,[a] and Reiner Anwander[a]*

[a] Institut für Anorganische Chemie, Eberhard Karls Universität Tübingen, Auf der Morgenstelle 18, 72076 Tübingen, Germany

[b] Department of Chemistry, University of Bergen, Allégaten 41, N-5007, Bergen, Norway

Corresponding Author

* reiner.anwander@uni-tuebingen.de

Table of Contents

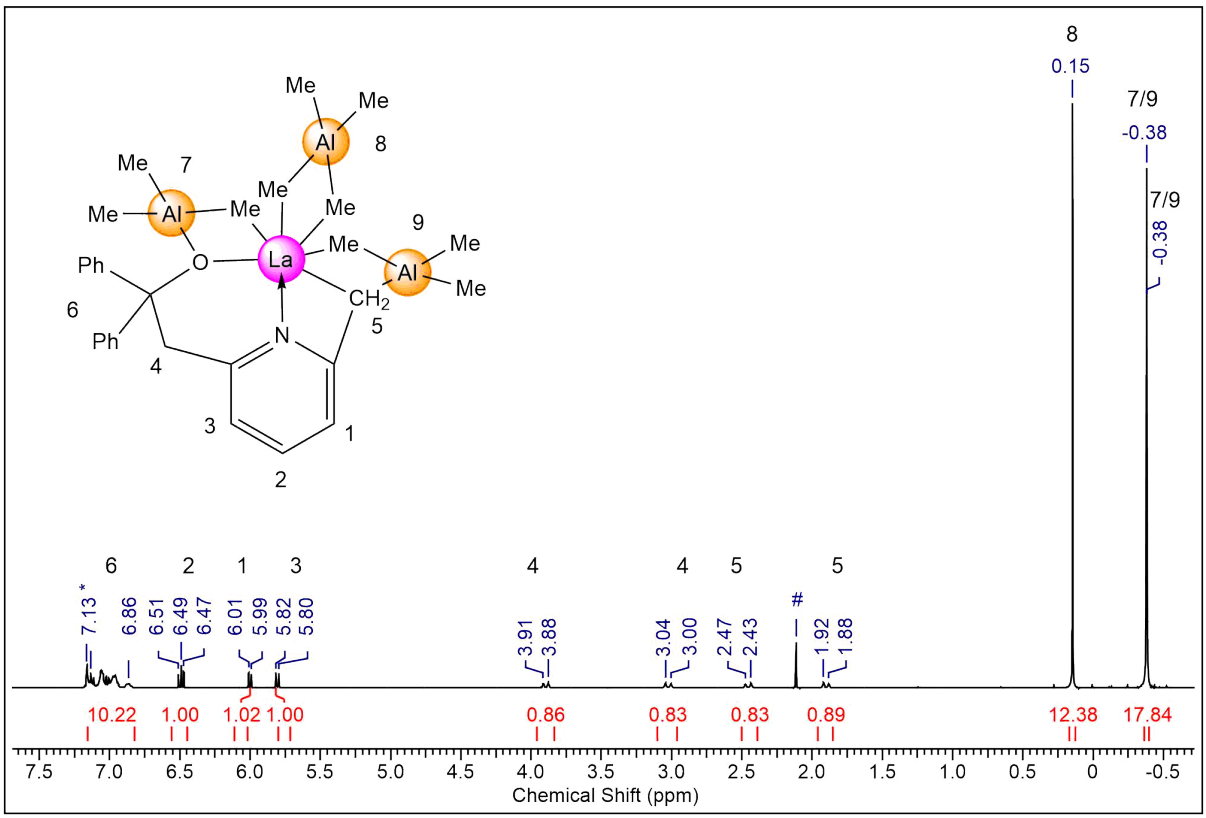

Figure S1. ^{1}H NMR spectrum (400 MHz) of $[ONCH_2]La(AlMe_3)_2(AlMe_4)$ (**2**^{La}) in C_6D_6 at 26 °C.

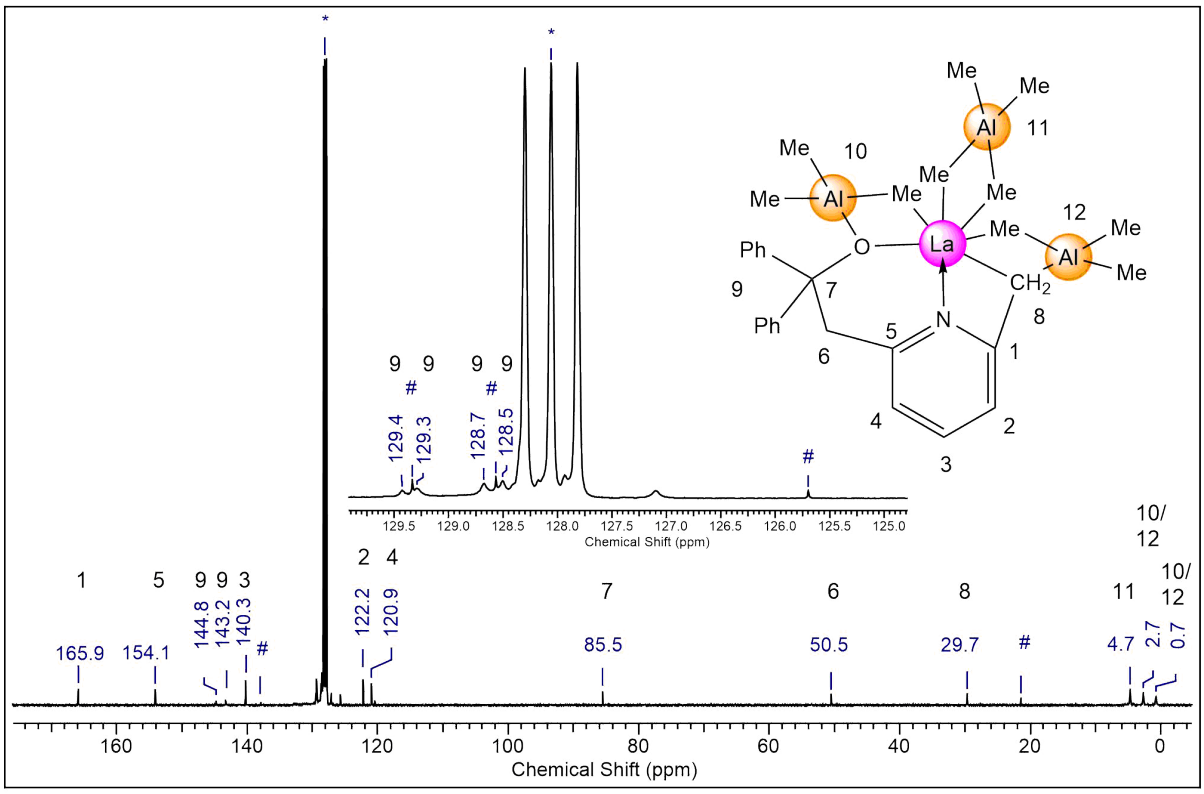

Figure S2. ^{13}C{^{1}H} spectrum (101 MHz) of $[ONCH_2]La(AlMe_3)_2(AlMe_4)$ (**2**^{La}) in C_6D_6 at 26 °C. Toluene is marked with #.

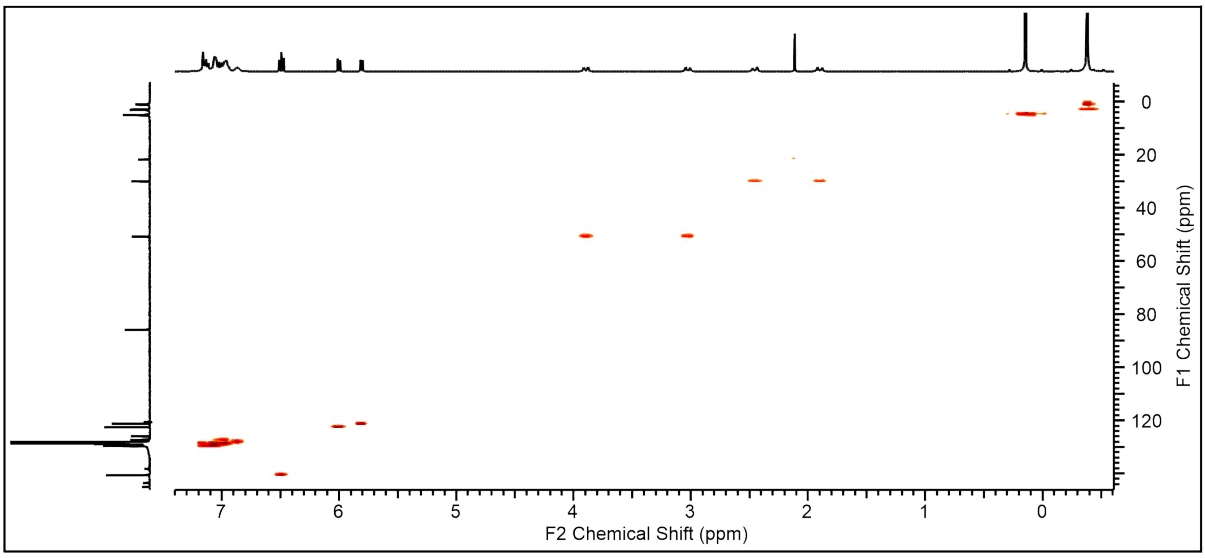

Figure S3. $^{1}H^{13}C$-HSQC NMR spectrum (400/101 MHz) of $[ONCH_2]La(AlMe_3)_2(AlMe_4)$ (**2**^{La}) in C_6D_6 at 26 °C.

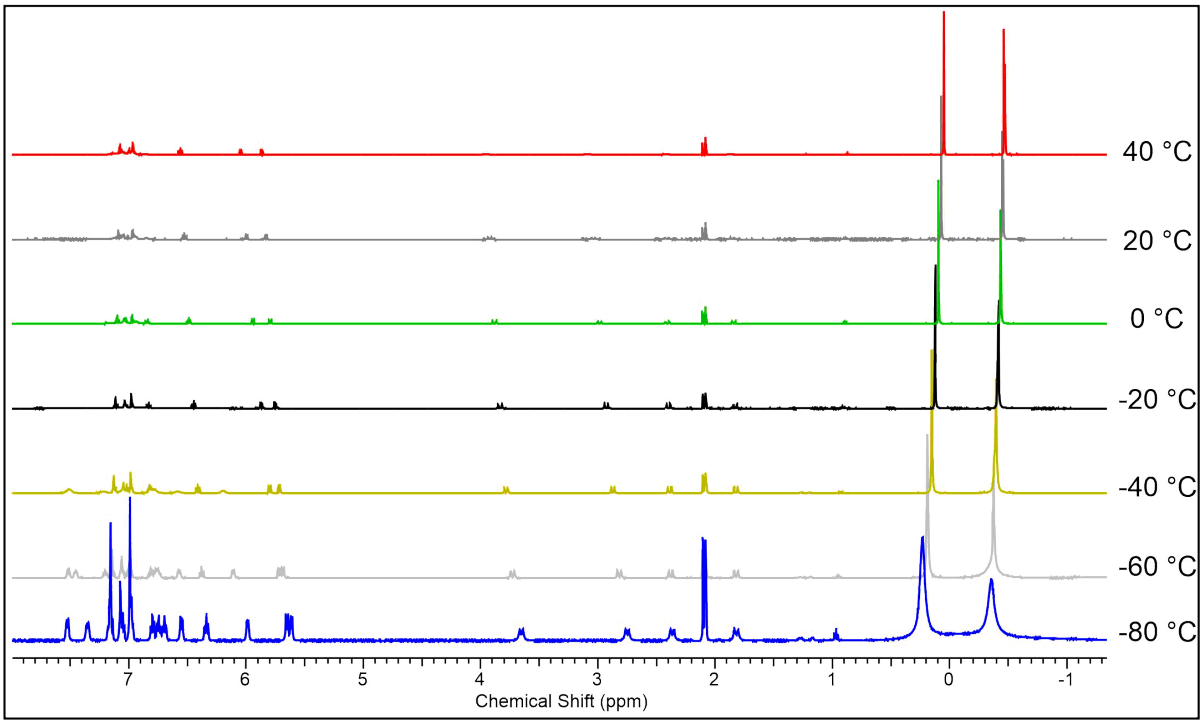

Figure S4. VT ^{1}H NMR spectra (500 MHz) of $[ONCH_2]La(AlMe_3)_2(AlMe_4)$ (**2**^{La}) in tolune-*d8*, in the range from –80 °C to 40 °C.

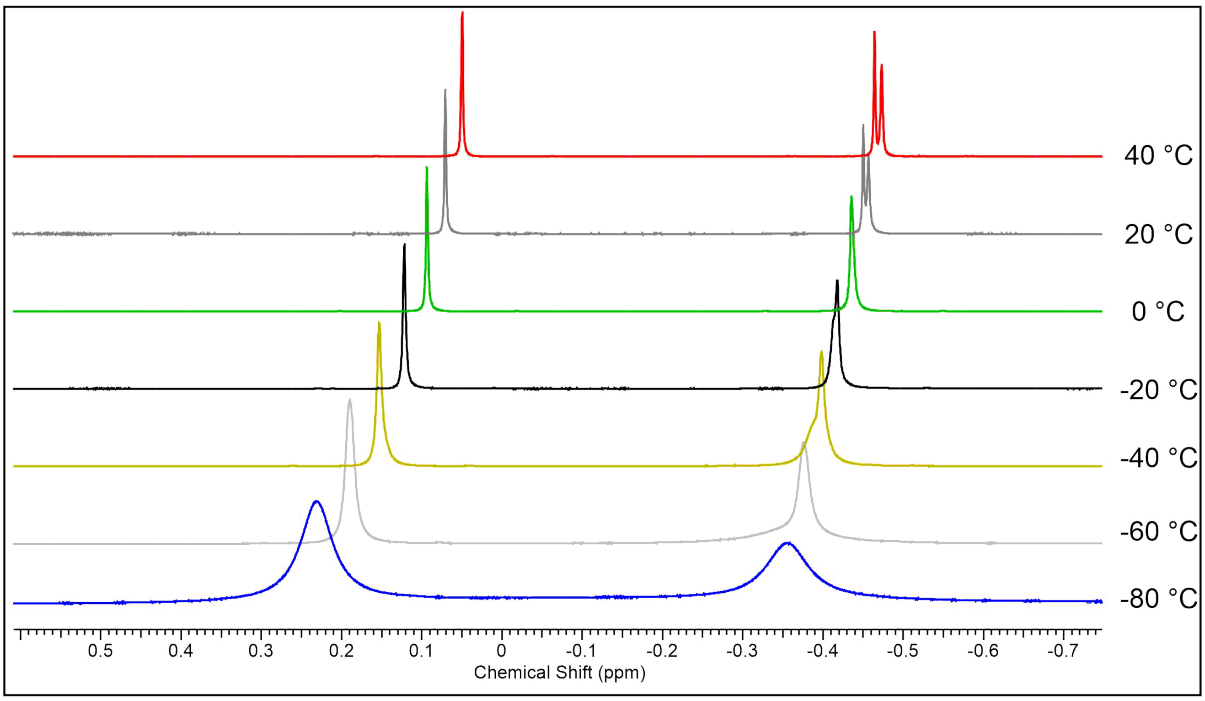

Figure S5. Detailed view of the VT ^{1}H NMR spectra (500 MHz) of $[ONCH_2]La(AlMe_3)_2(AlMe_4)$ (**2^{La}**) in tolune-*d8*, in the range from –80 °C to 40 °C.

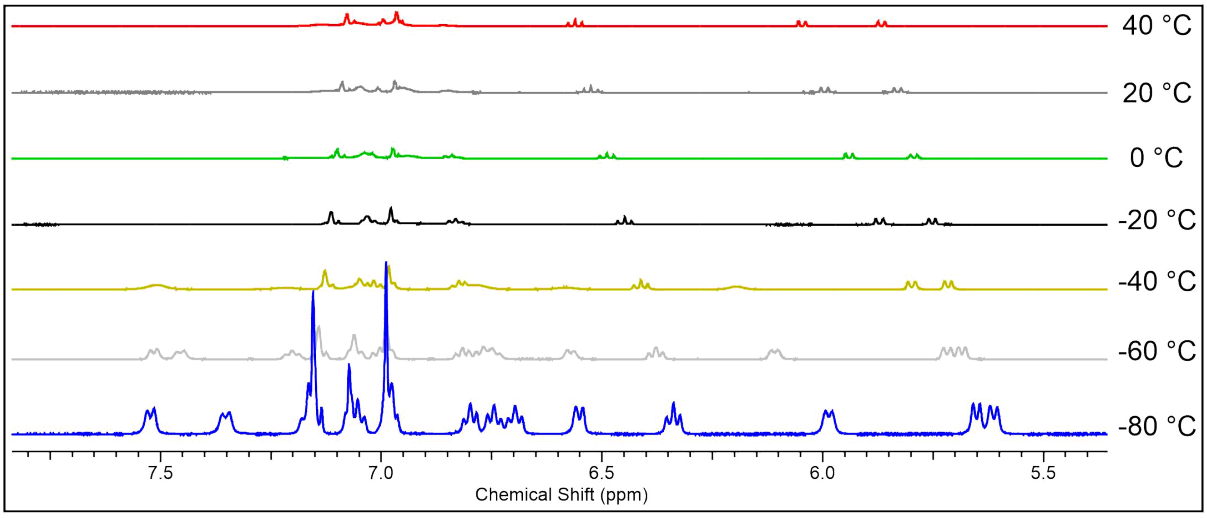

Figure S6. Detailed view of VT ^{1}H NMR spectra (500 MHz) of $[ONCH_2]La(AlMe_3)_2(AlMe_4)$ (**2^{La}**) in tolune-*d8*, in the range rrom –80 °C to 40 °C.

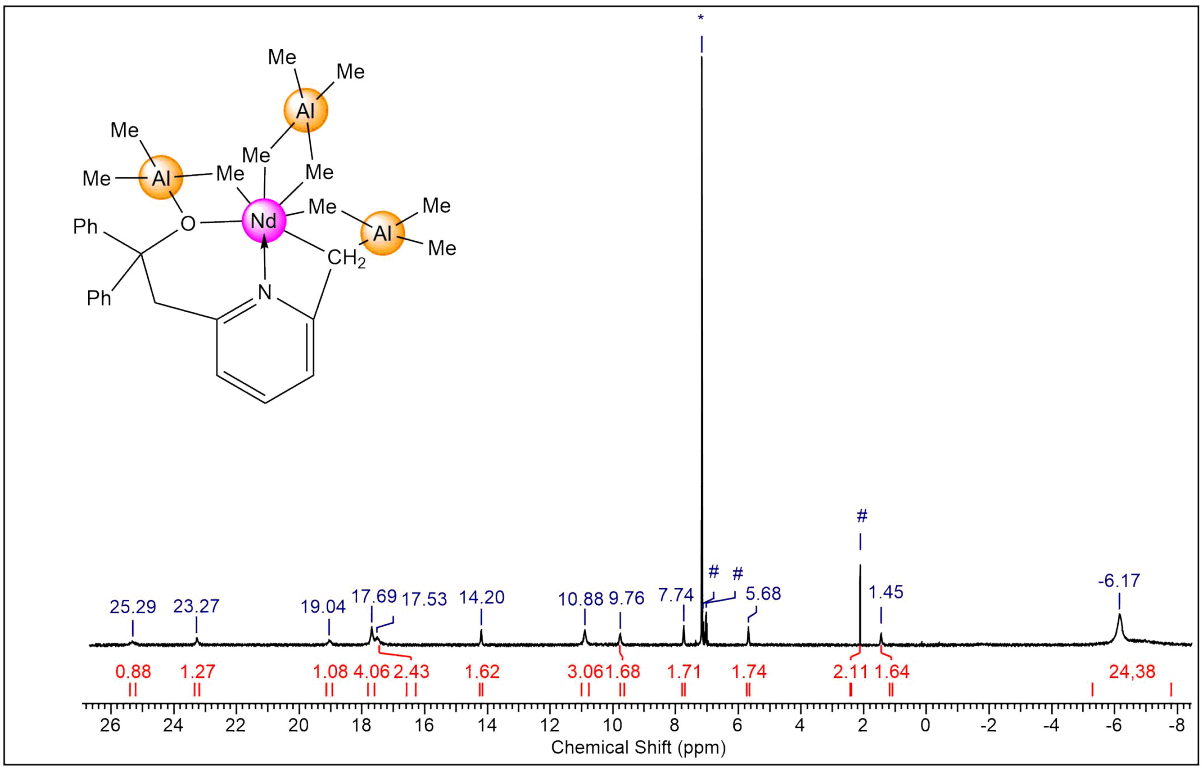

Figure S7. ^{1}H NMR spectrum (400 MHz) of $[ONCH_2]Nd(AlMe_3)_2(AlMe_4)$ (**2Nd**) in C_6D_6 at 26 °C. Toluene is marked with #.

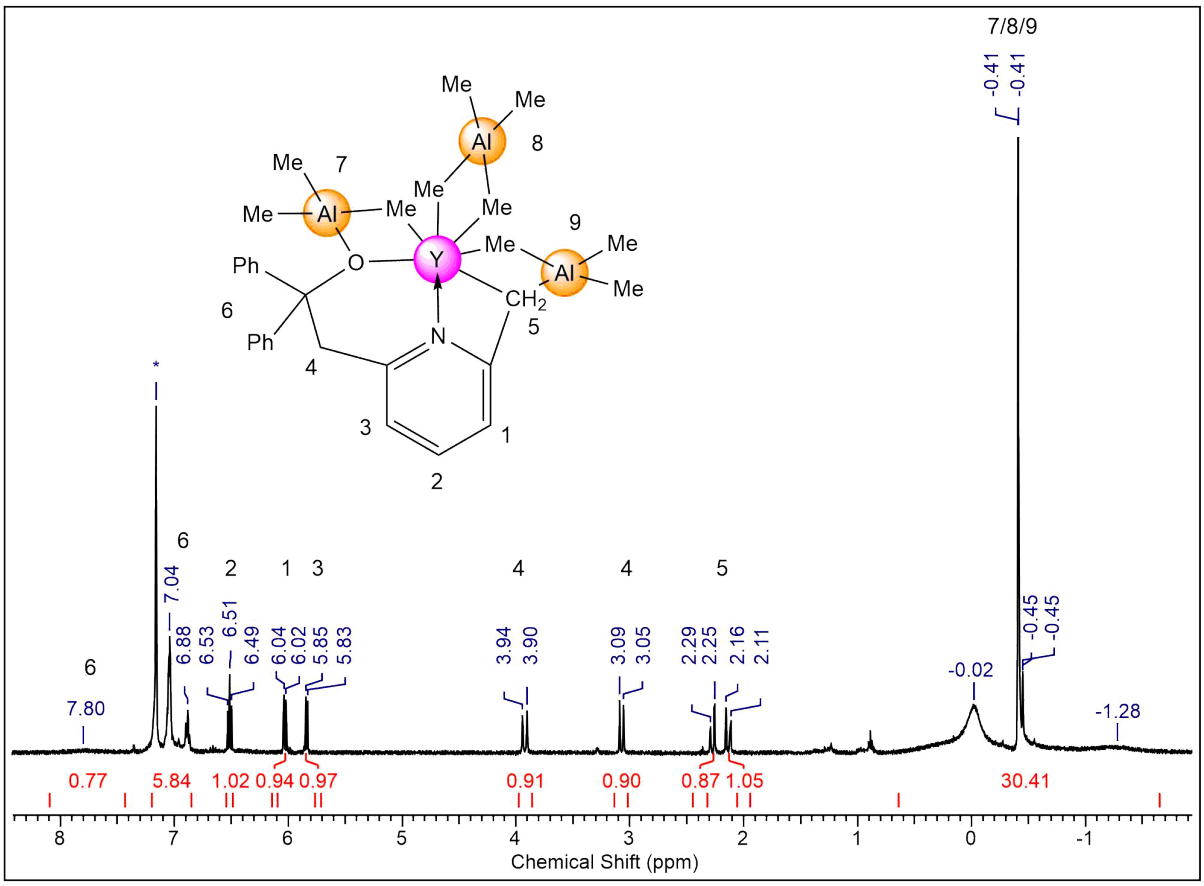

Figure S8. ^{1}H NMR spectrum (400 MHz) of $[ONCH_2]Y(AlMe_3)_2(AlMe_4)$ (**2^{Y}**) in C_6D_6 at 26 °C.

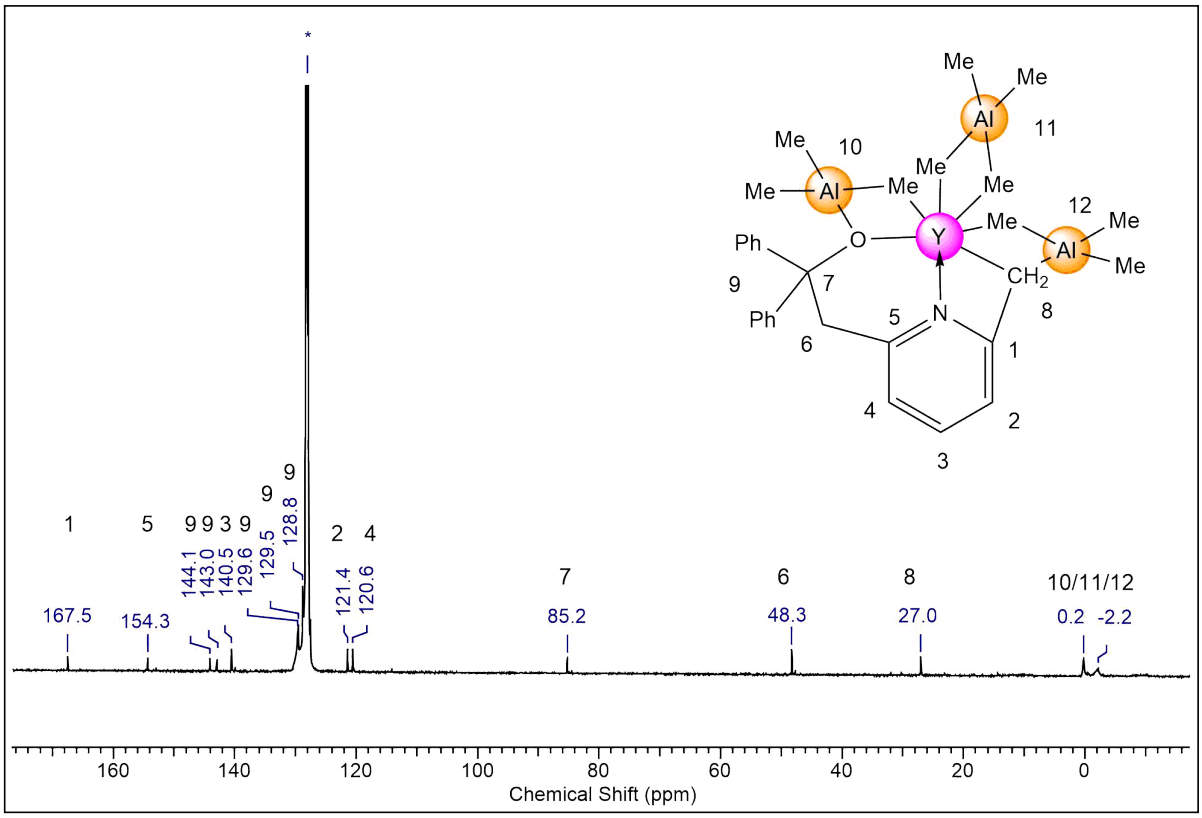

Figure S9. ^{13}C{^{1}H} spectrum (101 MHz) of $[ONCH_2]Y(AlMe_3)_2(AlMe_4)$ (**2^{Y}**) in C_6D_6 at 26 °C.

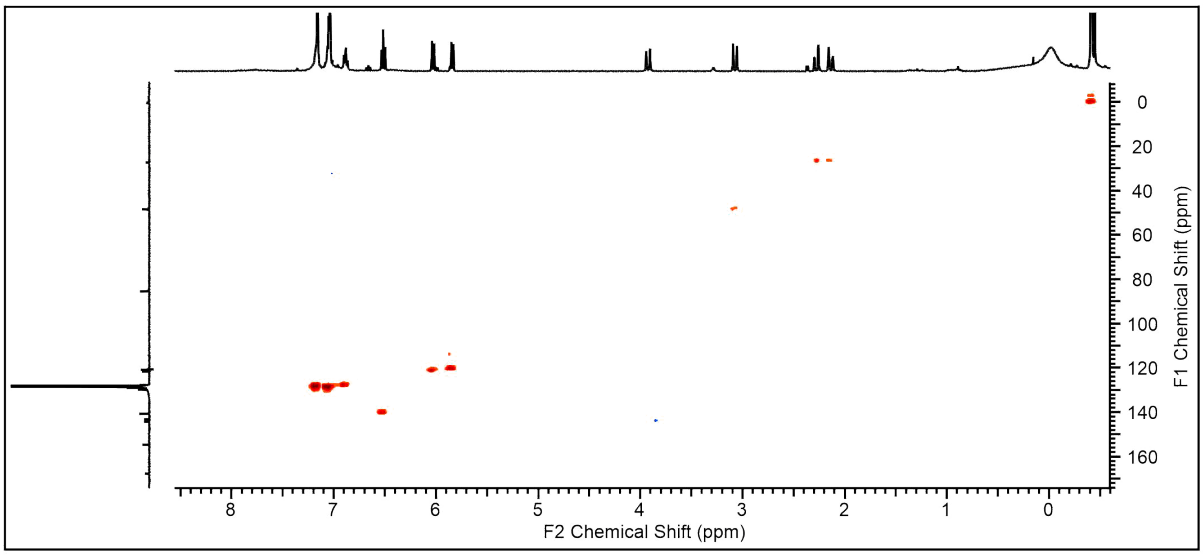

Figure S10. $^{1}H^{13}C$-HSQC NMR spectrum (400/101 MHz) of $[ONCH_2]Y(AlMe_3)_2(AlMe_4)$ (**2**^{Y}) in C_6D_6 at 26 °C.

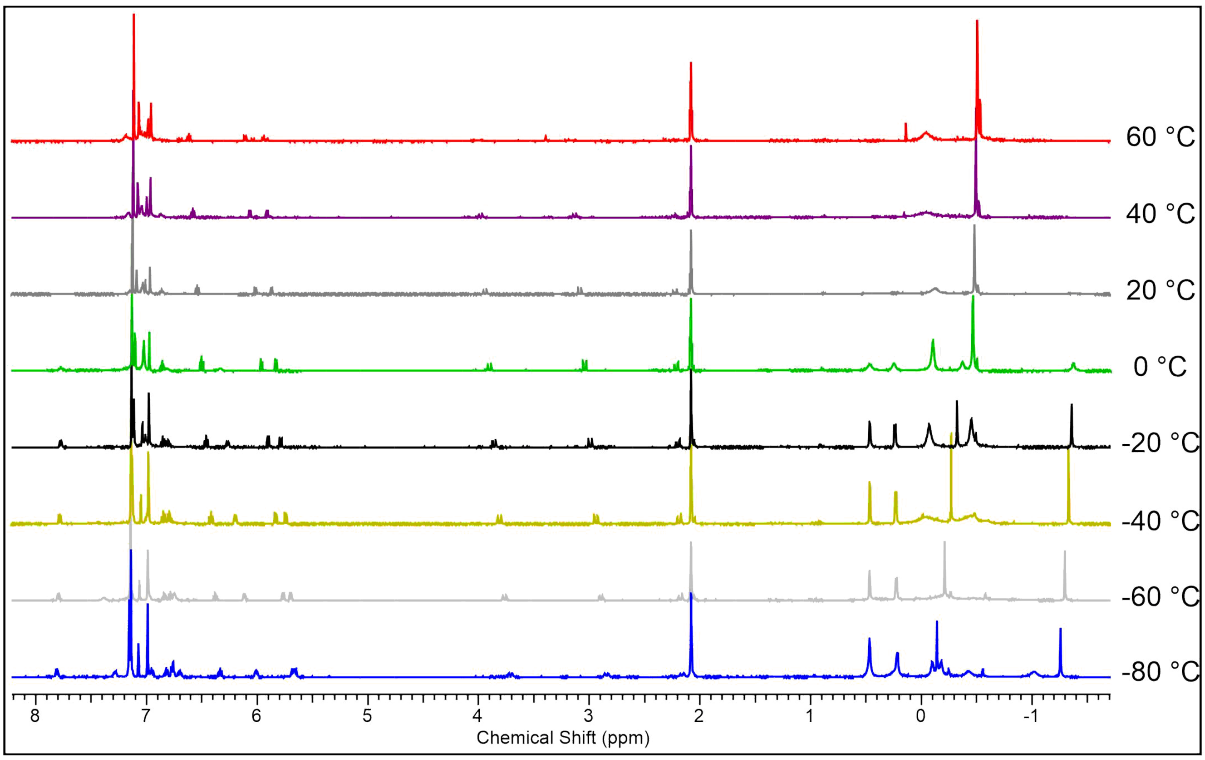

Figure S11. VT ^{1}H NMR spectra (500 MHz) of $[ONCH_2]Y(AlMe_3)_2(AlMe_4)$ (**2**^{Y}) in tolune-*d8*, in the range from –80 °C to 60 °C.

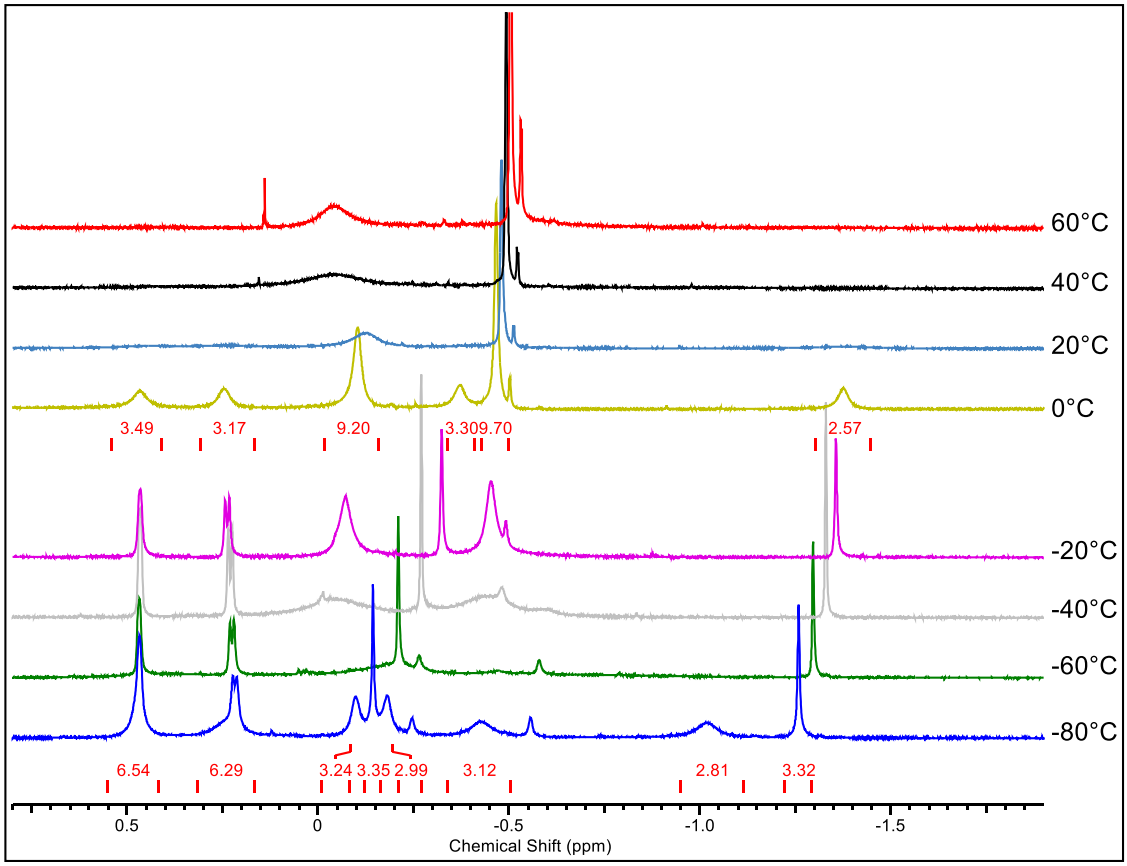

Figure S12. Detailed view of VT ^{1}H NMR spectra (500 MHz) of $[ONCH_2]Y(AlMe_3)_2(AlMe_4)$ (**2^Y**) in tolune-*d8*, in the range from –80 °C to 60 °C.

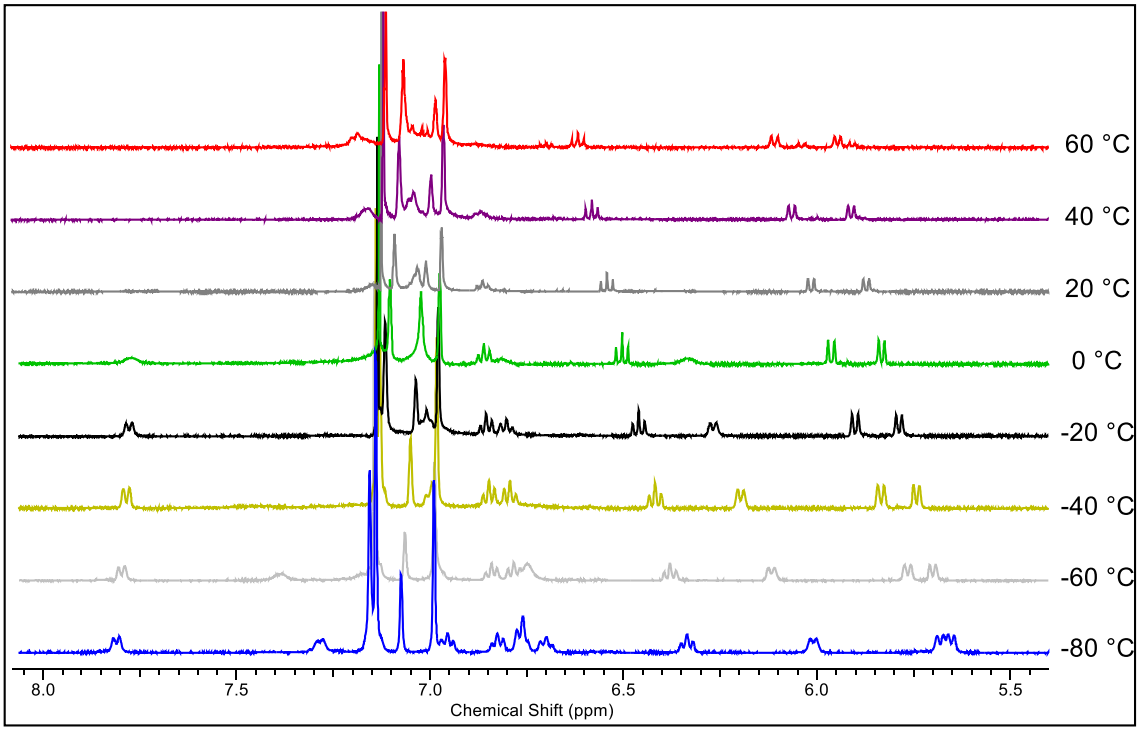

Figure S13. Detailed view of VT ^{1}H NMR spectra (500 MHz) of $[ONCH_2]Y(AlMe_3)_2(AlMe_4)$ (**2^Y**) in tolune-*d8*, in the range from –80 °C to 60 °C.

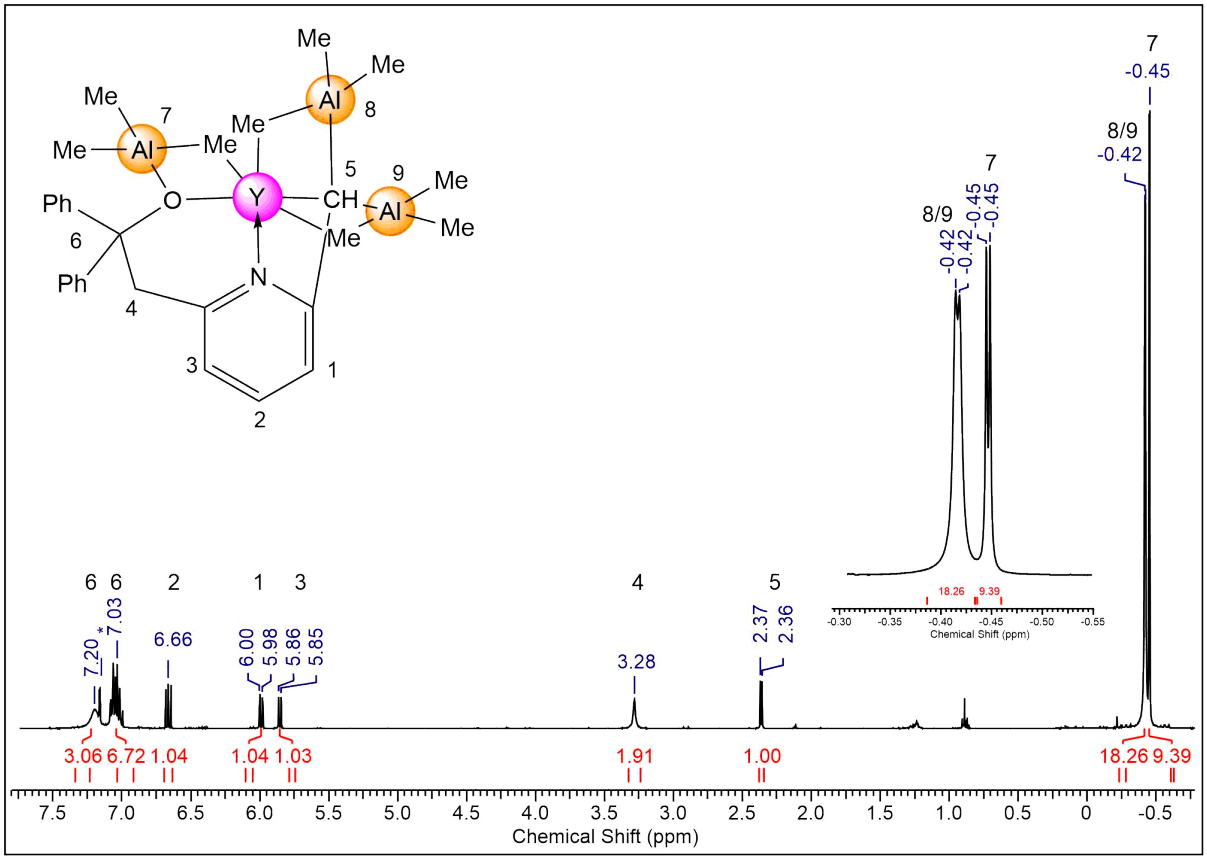

Figure S14. ^{1}H NMR spectrum (400 MHz) of [ONCH]Y(AlMe$_3$)$_3$ (**3^{Y}**) in C_6D_6 at 26 °C.

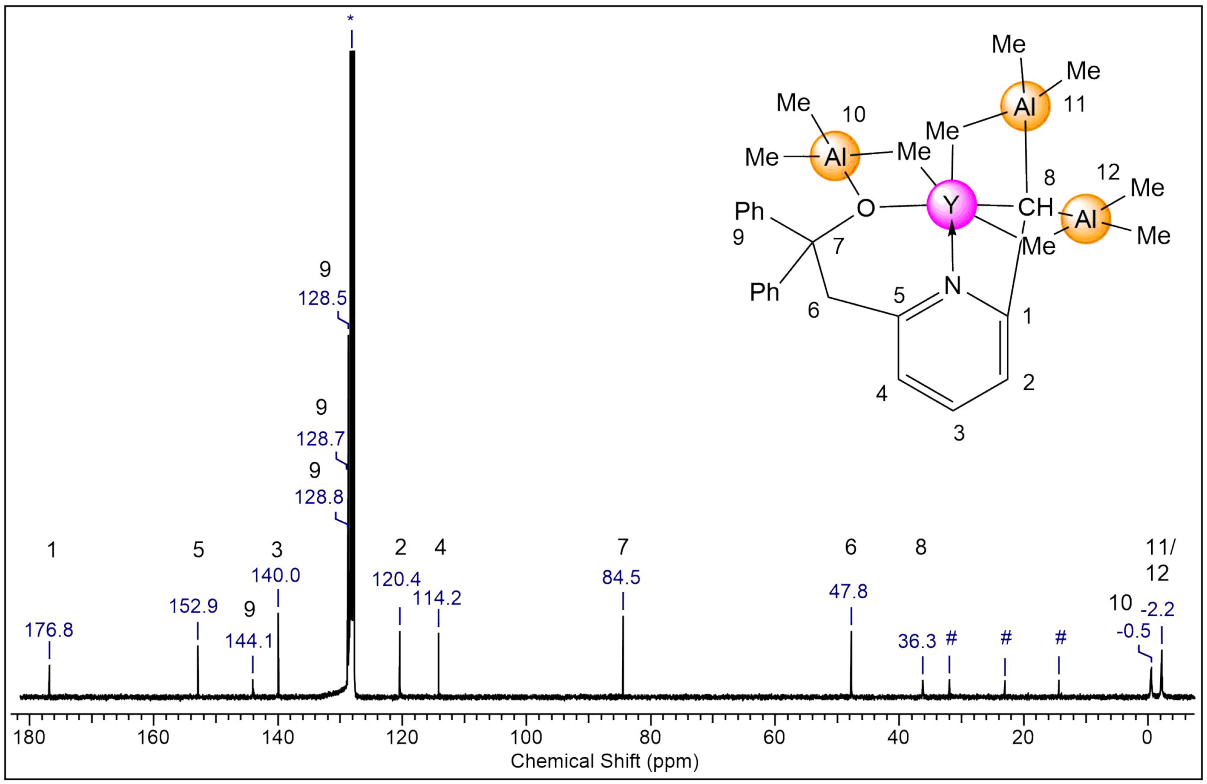

Figure S15. ^{13}C{^{1}H} spectrum (101 MHz) of [ONCH]Y(AlMe$_3$)$_3$ (**3^{Y}**) in C_6D_6 at 26 °C. *n*-Hexane is marked with #.

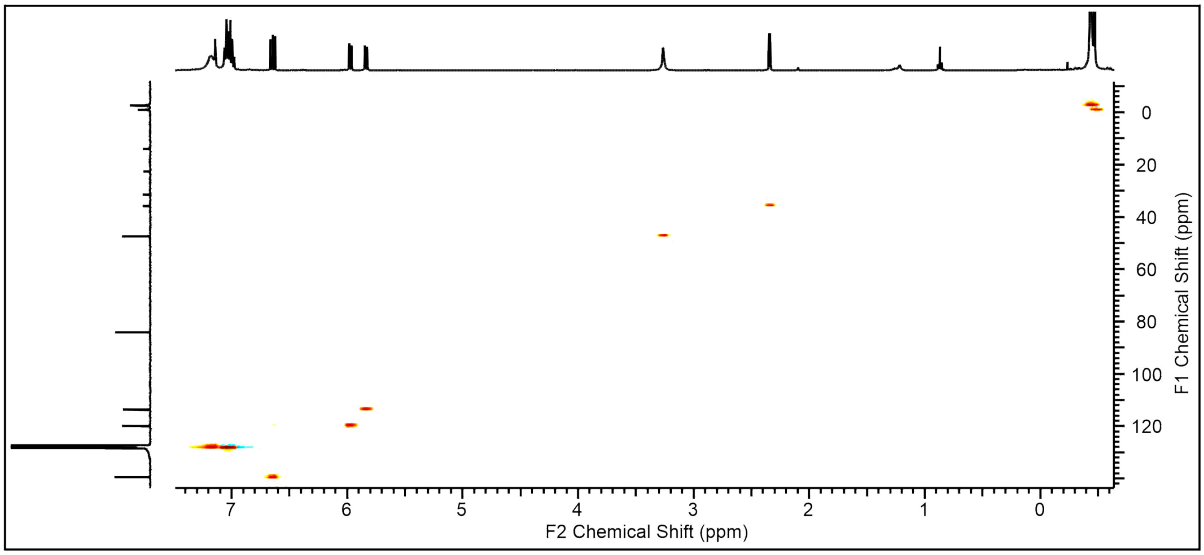

Figure S16. $^{1}H^{13}C$-HSQC NMR spectrum (400/101 MHz) of [ONCH]Y($AlMe_3$)$_3$ (**3**^{Y}) in C_6D_6 at 26 °C.

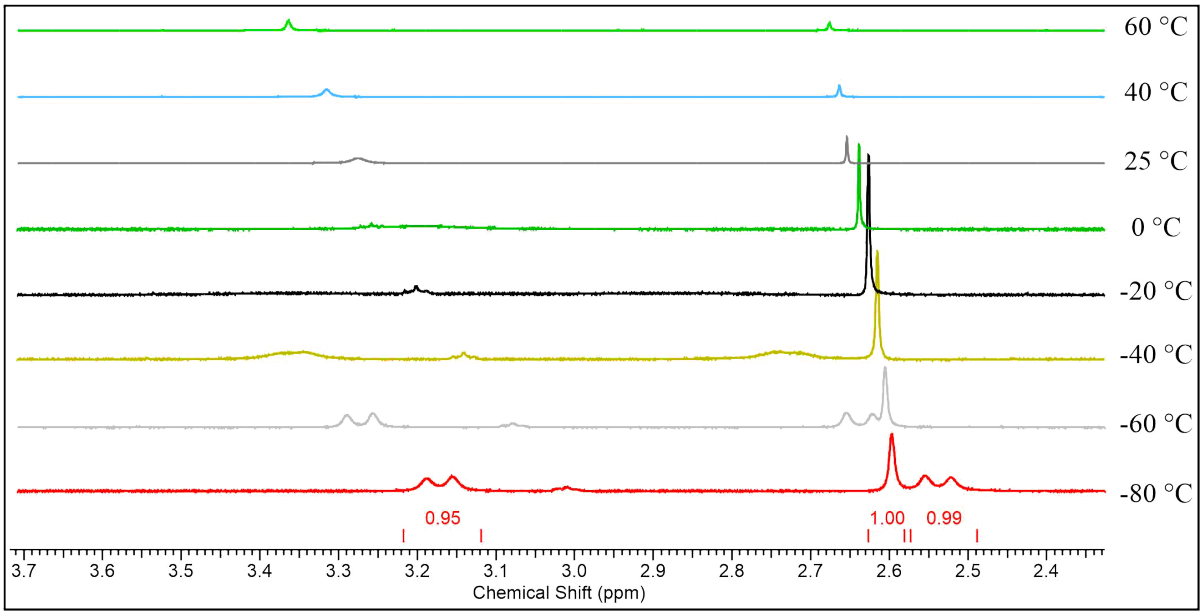

Figure S17. Detailed view of VT ^{1}H NMR spectra (500 MHz) of [ONCH]Y($AlMe_3$)$_3$ (**3**^{Y}) in tolune-*d8*, in the range from –80 °C to 60 °C.

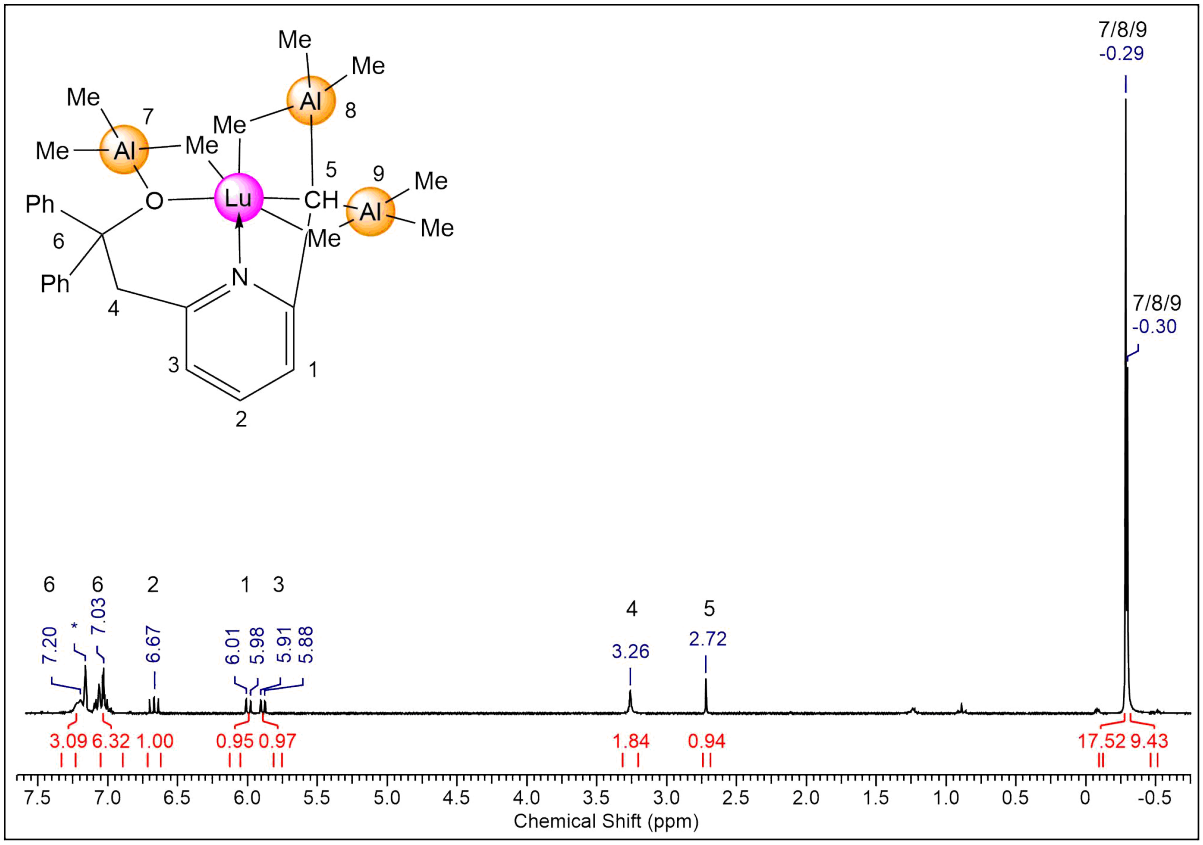

Figure S18. ^{1}H NMR spectrum (400 MHz) of [ONCH]Lu(AlMe$_3$)$_3$ (**3^{Lu}**) in C_6D_6 at 26 °C.

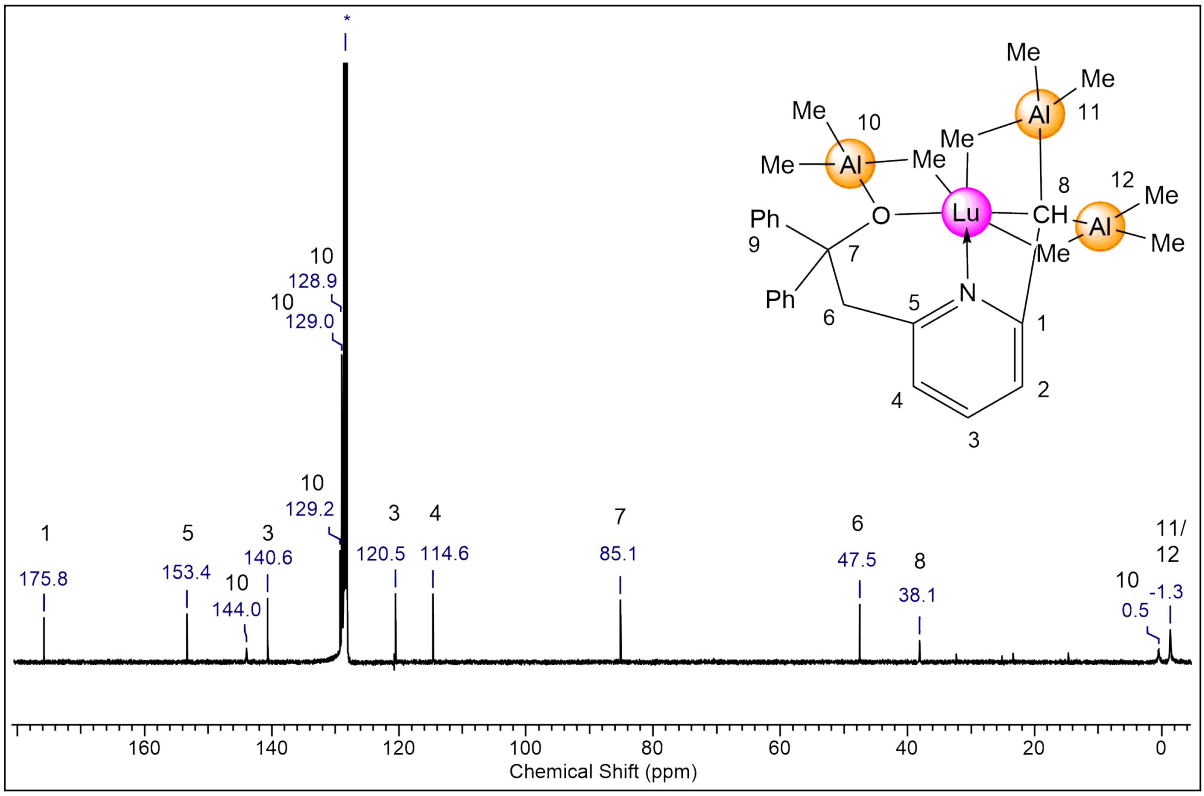

Figure S19. ^{13}C{^{1}H} spectrum (101 MHz) of [ONCH]Lu(AlMe$_3$)$_3$ (**3^{Lu}**) in C_6D_6 at 26 °C.

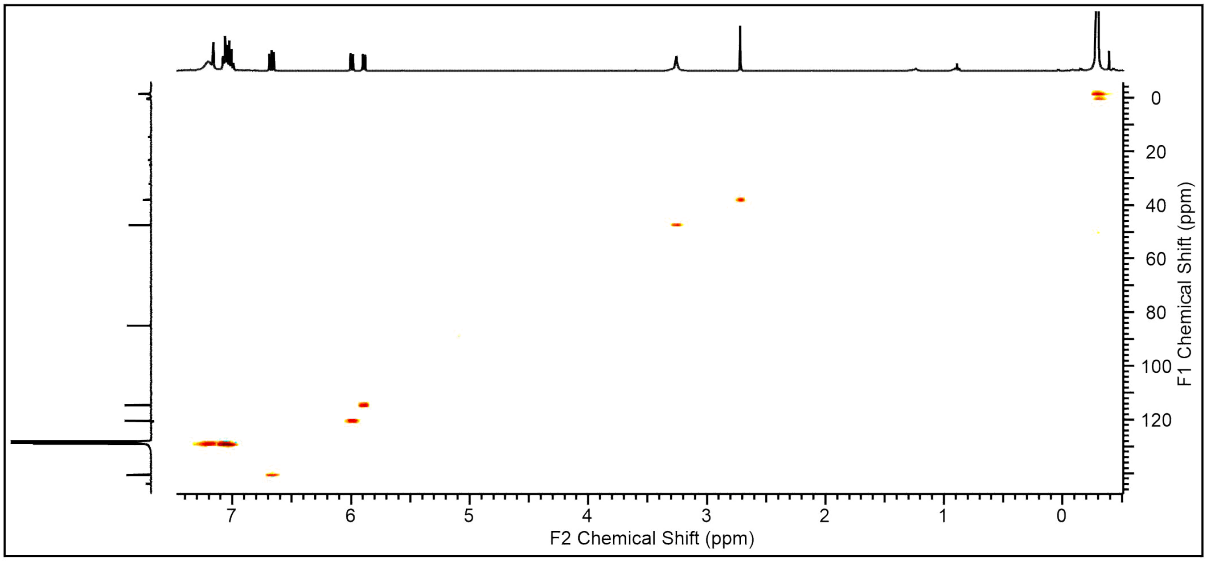

Figure S20. $^{1}H^{13}C$-HSQC NMR spectrum (400/101 MHz) of [ONCH]Lu($AlMe_3$)$_3$ (**3^{Lu}**) in C_6D_6 at 26 °C.

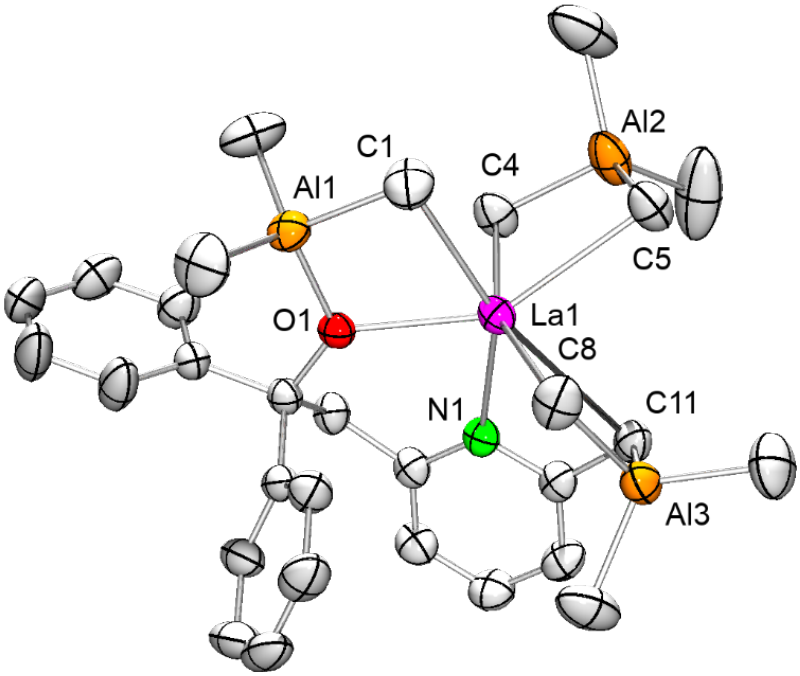

Figure S21. Crystal structure of [ONCH$_2$]La(AlMe$_3$)$_2$(AlMe$_4$) (**2^{La}**). Hydrogen atoms are omitted for clarity. The asymmetric unit contains 0.5 toluene which is omitted for clarity. Atomic displacement parameters set at the 50% probability level. Selected bond lengths [Å] and angles [°]: La1–C1 2.726(2), La1–C4 2.688(2), La1–C5 2.787(2), La1–C8 2.720(2), La1–C11 2.949(2), La1···Al1 3.3509(5), La1···Al2 3.2827(6), La1···Al3 3.4013(5), La1–N1 2.517(1), La1–O1 2.412(1), Al1–O1 1.862(1), Al3–C11 2.092(2), O1-La1-C11 126.21(4), O1-La1-N1 76.37(4), N1-La1-C11 51.40(4), N1-La1-Al2 107.20(3).

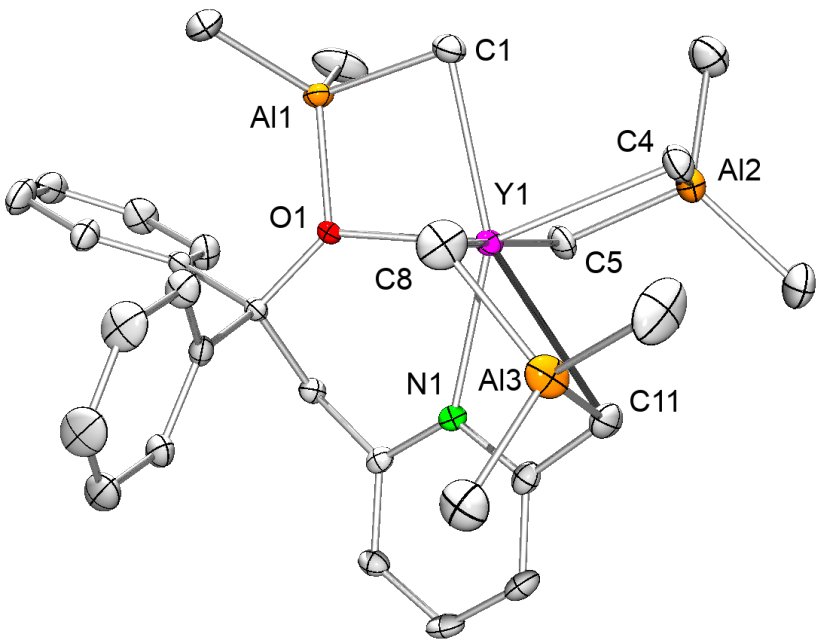

Figure S22. Crystal structure of $[ONCH_2]Y(AlMe_3)_2(AlMe_4)$ (**2**^{Y}). Hydrogen atoms are omitted for clarity. The asymmetric unit contains 0.5 toluene which is omitted for clarity. Atomic displacement parameters set at the 50% probability level. Selected bond lengths [Å] and angles [°]: Y1–C1 2.583(3), Y1–C4 2.518(3), Y1–C5 2.677(3), Y1–C8 2.513(4), Y1–C11 2.848(3), Y1···Al1 3.1934(8), Y1···Al2 3.1390(9), Y1···Al3 3.251(1), Y1–N1 2.386(2), Y1–O1 2.270(2), Al1–O1 1.851(2), Al3–C11 2.070(3), O1-Y1-C11 130.21(7), O1-Y1-N1 78.70(6), N1-Y1-C11 53.16(8), N1-Y1-Al2 108.75(5).

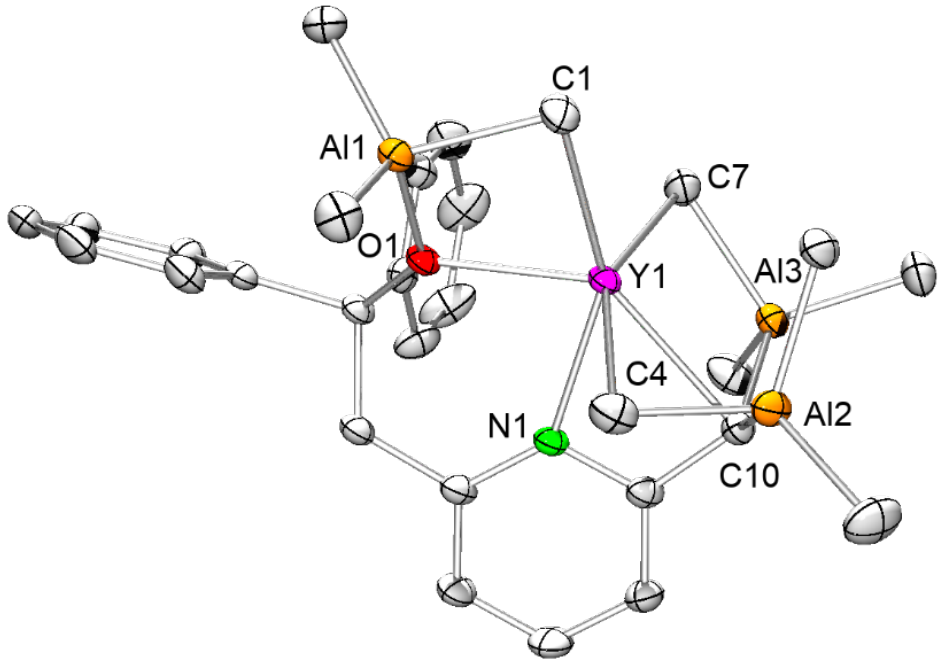

Figure S23. Crystal structure of $[ONCH]Y(AlMe_3)_3$ (**3**^{Y}). Hydrogen atoms are omitted for clarity. The asymmetric unit contains one toluene which was omitted for clarity. Atomic displacement parameters set at the 50% probability level. Selected bond lengths [Å] and angles [°]: Y1–C1 2.568(2), Y1–C4 2.640(2), Y1–C7 2.483(2), Y1–C10 2.611(2), Y1···Al1 3.1899(6), Y1···Al2 2.8420(6), Y1···Al3 3.1295(6), Y1–N1 2.325(1), Y1–O1 2.270(1), Al1–O1 1.849(1), Al2–C10 2.052(2), Al3–C10 2.063(2), O1-Y1-C10 134.96(5), O1-Y1-N1 75.10(5), N1-Y1-C10 56.92(5).

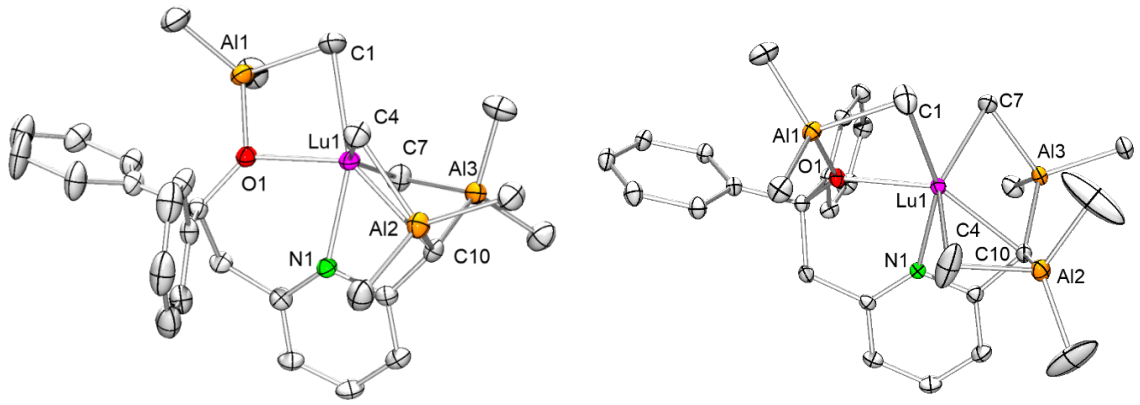

Figure S24. Crystal structures of [ONCH]Lu($AlMe_3$)$_3$ (left: $\mathbf{3^{Lu}}$, right $\mathbf{3^{Lu*}}$). Hydrogen atoms are omitted for clarity. Atomic displacement parameters set at the 50% probability level. Selected bond lengths [Å] and angles [°]: $\mathbf{3^{Lu}}$: Lu1–C1 2.511(3), Lu1–C4 2.580(3), Lu1–C7 2.436(3), Lu1–C10 2.524(3), Lu1···Al1 3.1221(9), Lu1···Al2 2.8623(8), Lu1···Al3 3.0575(9), Lu1–N1 2.281(2), Lu1–O1 2.193(2), Al1–O1 1.848(2), Al2–C10 2.076(3), Al3–C10 2.073(3), O1-Lu1-C10 136.27(8), O1-Lu1-N1 78.38(7), N1-Lu1-C10 58.33(9). $\mathbf{3^{Lu*}}$: Lu1–C1 2.550(2), Lu1–C4 2.508(2), Lu1–C7 2.440(2), Lu1–C10 2.526(2), Lu1···Al1 3.1082(6), Lu1···Al2 2.9630(6), Lu1···Al3 3.0479(6), Lu1–N1 2.277(2), Lu1–O1 2.187(1), Al1–O1 1.851(1), Al2–C10 2.082(2), Al3–C10 2.063(2), O1-Lu1-C10 136.56(5), O1-Lu1-N1 78.69(5), N1-Lu1-C10 58.43(6).

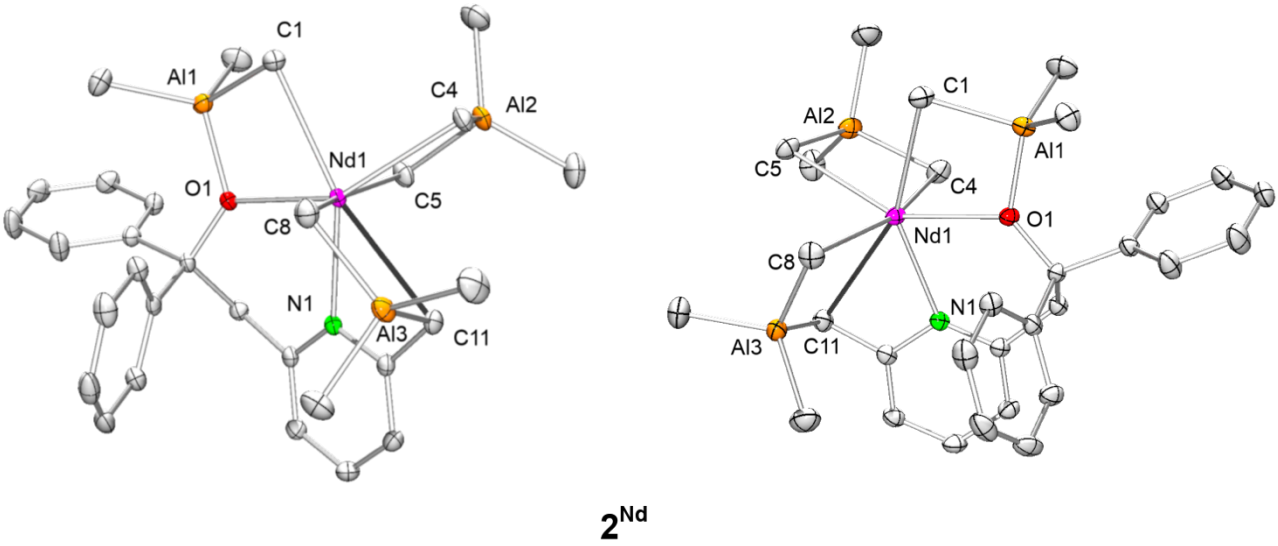

Figure S25. Comparison of both enantiomers of the crystal structure of $\mathbf{2^{Nd}}$.

Table S1. Crystallographic data for compounds $\mathbf{2^{La}}$, $\mathbf{2^{Nd}}$, and $\mathbf{2^{Y}}$

	$\mathbf{2^{La}}$	$\mathbf{2^{Nd}}$	$\mathbf{2^{Y}}$
CCDC	1971551	1971552	1971555
formula	$C_{33.5}H_{51}Al_3LaNO$	$C_{33.5}H_{51}Al_3NdNO$	$C_{33.5}H_{51}Al_3YNO$
M [g·mol^{-1}]	703.60	708.93	653.60
Color	yellow	blue/green	yellow
Crystal dimensions [mm]	0.52 x 0.45 x 0.28	0.242 x 0.214 x 0.165	0.197 x 0.183 x 0.070
Crystal system	triclinic	triclinic	monoclinic
space group	$P\bar{1}$	$P\bar{1}$	$P2_1/c$
a [Å]	10.3933(4)	10.6177(3)	17.8953(13)
b [Å]	11.9336(4)	11.4277(4)	10.0184(8)
c [Å]	15.6945(6)	16.3857(4)	20.9266(15)
α [°]	87.3861(4)	93.045(2)	90
β [°]	85.6753(4)	99.2350(10)	109.621(3)
γ [°]	72.0755(4)	112.8170(10)	90
V [Å^3]	1846.32(12)	1794.24(9)	3533.9(5)
Z	2	2	4
T [K]	200(2)	100(2)	100(2)
ρ_{calcd} [g·cm^{-3}]	1.266	1.312	1.228
μ [mm^{-1}]	1.252	1.545	1.749
F(000)	726	732	1380
Unique reflns	10787	8887	7791
Observed reflns (I>2σ)	31465	31707	56238
R1/*w*R2 (I>2σ)	0.0229/0.0589	0.0233/0.0580	0.0450/0.0980
R1/*w*R2 (all data)	0.0255/0.0611	0.0260/0.0596	0.0566/0.1017
Goodness of fit	1.075	1.034	1.121

Table S2. Crystallographic data for compounds $\mathbf{3^{Y}}$, $\mathbf{3^{Lu}}$ and $\mathbf{3^{Lu*}}$

	$\mathbf{3^{Y}}$	$\mathbf{3^{Lu}}$	$\mathbf{3^{Lu*}}$
CCDC	1971553	1971554	1977635
formula	$C_{35}H_{55}Al_3YNO$	$C_{29}H_{43}Al_3LuNO$	$C_{29}H_{43}Al_3LuNO$
M [g·mol^{-1}]	675.65	677.55	677.55
Color	yellow	yellow	yellow
Crystal dimensions [mm]	0.425 x 0.348 x 0.238	0.132 x 0.124 x 0.104	0.400 x 0.125 x 0.050
cell	triclinic	monoclinic	orthorhombic
space group	$P\bar{1}$	$P2_1/n$	$P2_12_12_1$
a [Å]	10.3672(4)	11.1015(9)	10.6476(4)
b [Å]	12.9566(5)	21.7863(18)	13.3042(6)
c [Å]	14.9981(6)	13.0879(10)	22.2103(9)
α [°]	99.106(2)	90	90
β [°]	95.286(2)	104.7510(10)	90
γ [°]	109.956(2)	90	90
V [Å^3]	1846.44(13)	3061.1(4)	3146.3(2)
Z	2	4	4
T [K]	100(2)	150(2)	103(2)
ρ_{calcd} [g·cm^{-3}]	1.215	1.470	1.430
μ [mm^{-1}]	1.676	3.332	3.242
F(000)	716	1368	1368
Unique reflns	8139	9386	10781
Observed reflns (I>2σ)	74275	48629	10653
R1/*w*R2 (I>2σ)	0.0307/0.0798	0.0303/0.0545	0.0121/0.0321
R1/*w*R2 (all data)	0.0333/0.0817	0.0488/0.0612	0.0123/0.0322
Goodness of fit	1.028	1.019	1.043

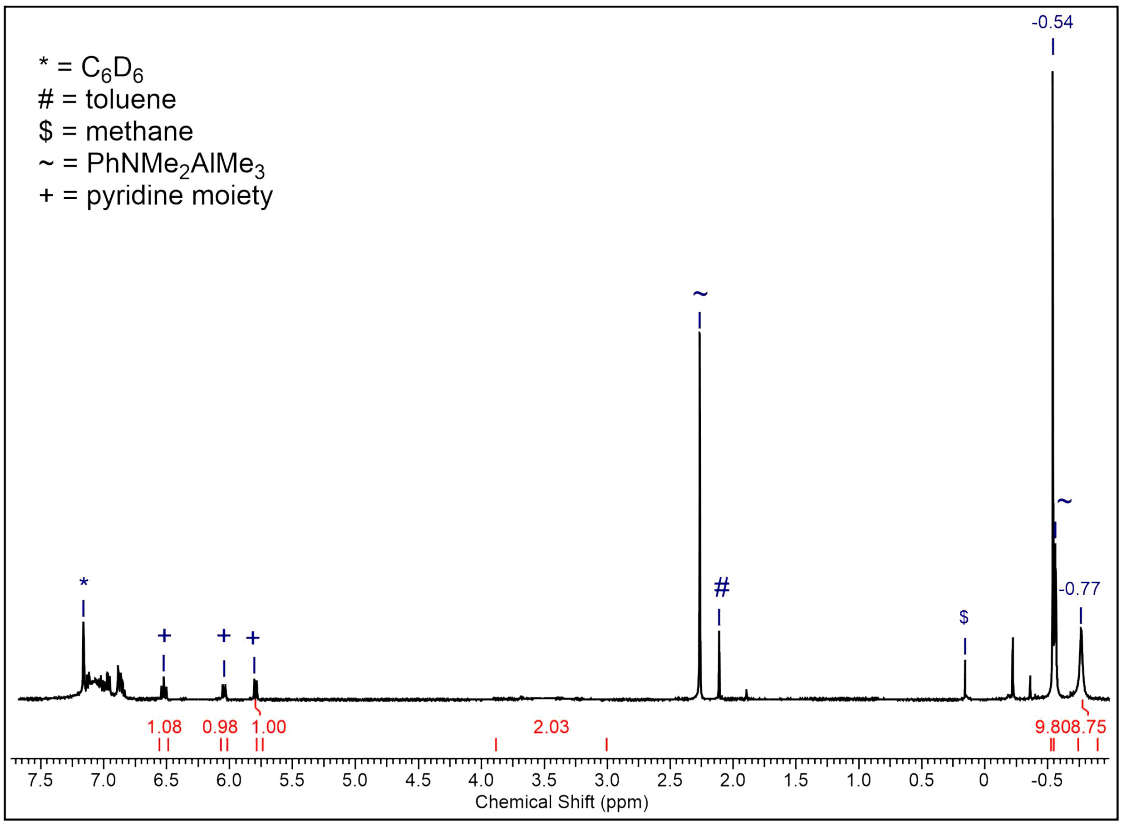

Figure S26. ^{1}H NMR spectrum (400 MHz) of the reaction of $[ONCH_2]La(AlMe_3)_2(AlMe_4)$ (**2**^{La}) with $[Ph_3C][B(C_6F_5)_4]$ in C_6D_6 at 26 °C.

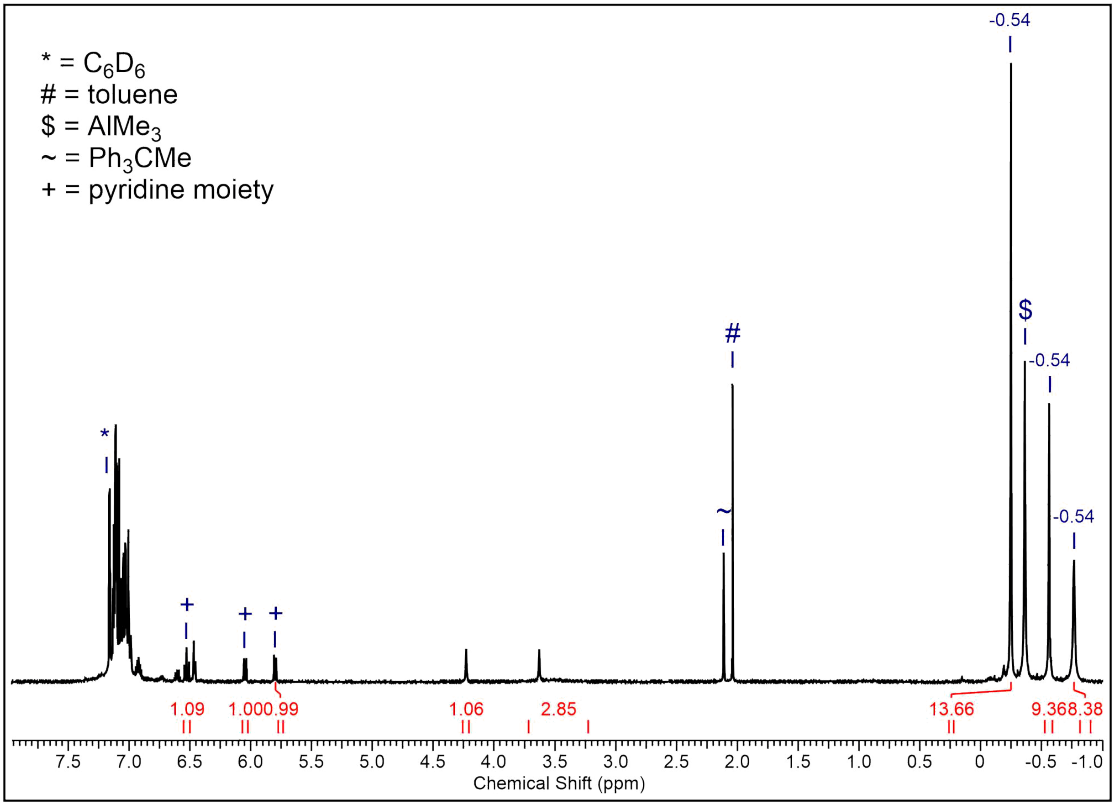

Figure S27. ^{1}H NMR spectrum (400 MHz) of the reaction of $[ONCH_2]La(AlMe_3)_2(AlMe_4)$ (**2**^{La}) with $[PhNMe_2H][B(C_6F_5)_4]$ in C_6D_6 at 26 °C.

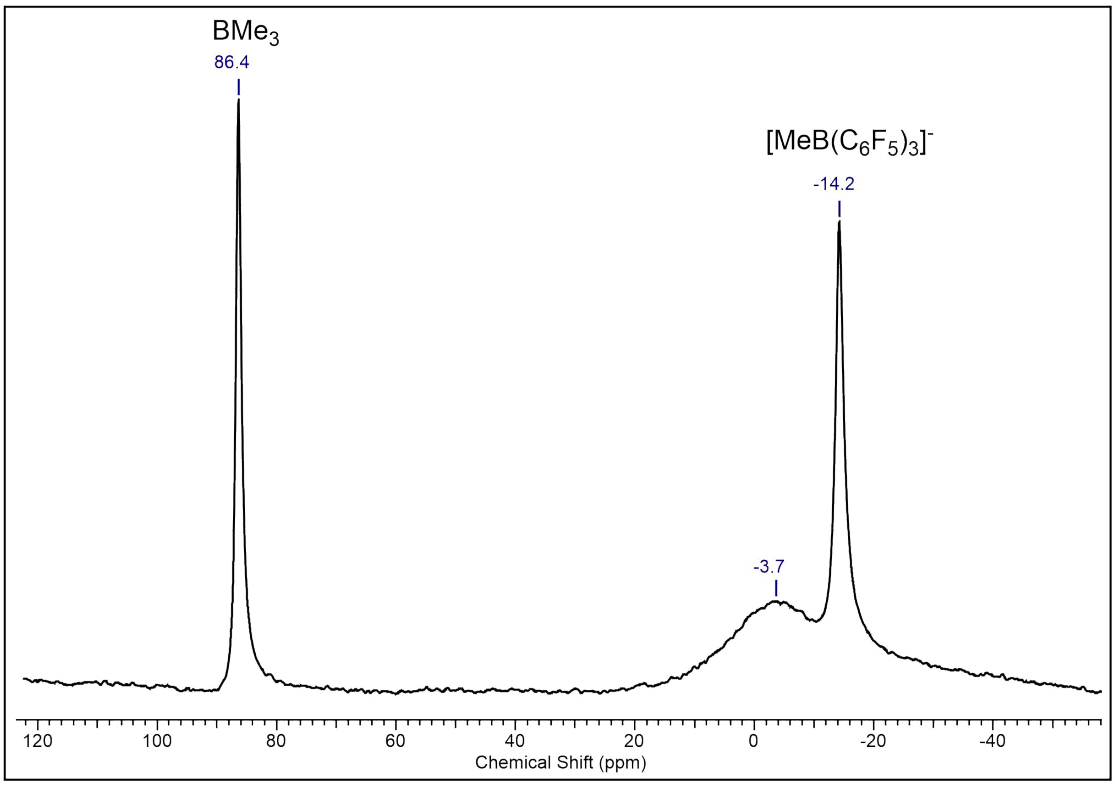

Figure S28. $^{11}B\{^1H\}$ NMR spectrum (96 MHz) of the reaction of $[ONCH_2]La(AlMe_3)_2(AlMe_4)$ (**2**^{La}) with $B(C_6F_5)_3$ in C_6D_6 at 25 °C.

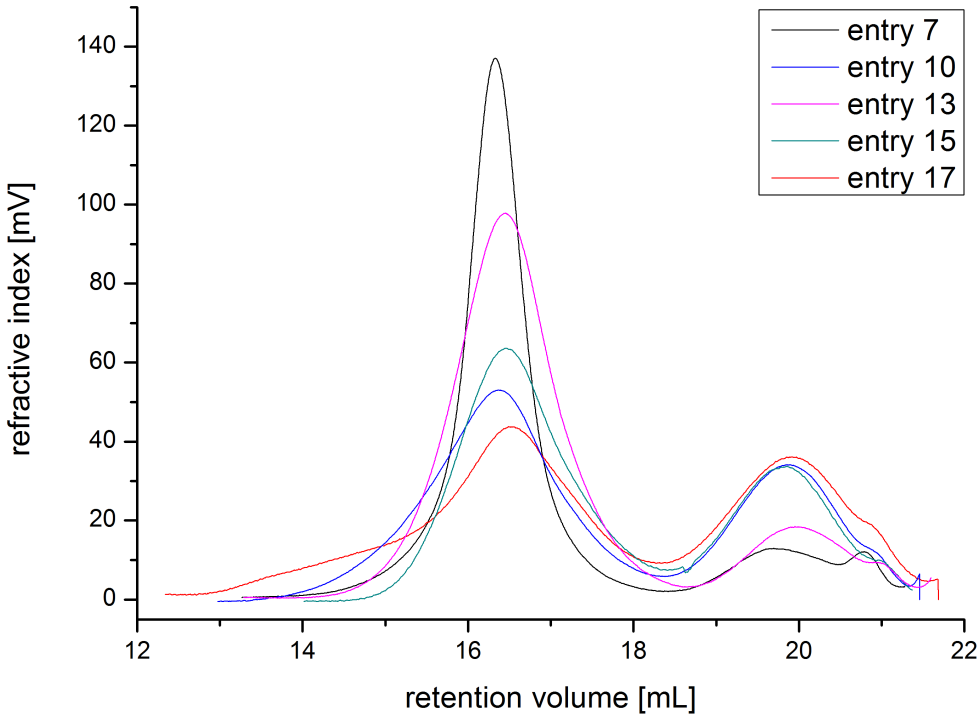

Figure S29. Refractive index (RI) of bimodalic polyisoprenes (Table 2, entries 7, 10, 13, 15, and 17).